Baroclinic control of Southern Ocean eddy-driven upwelling near topography

- insights from idealized simulations and energetics -

Alice Barthel (LANL)

Andy Hogg (ANU), Stephanie Waterman (UBC),

Shane Keating (UNSW)

Los Alamos NATIONAL LABORATORY EST. 1943

LA-UR-18-20999

UNSW THE UNIVERSITY OF NEW SOUTH WALES

EKE and upwelling near topography

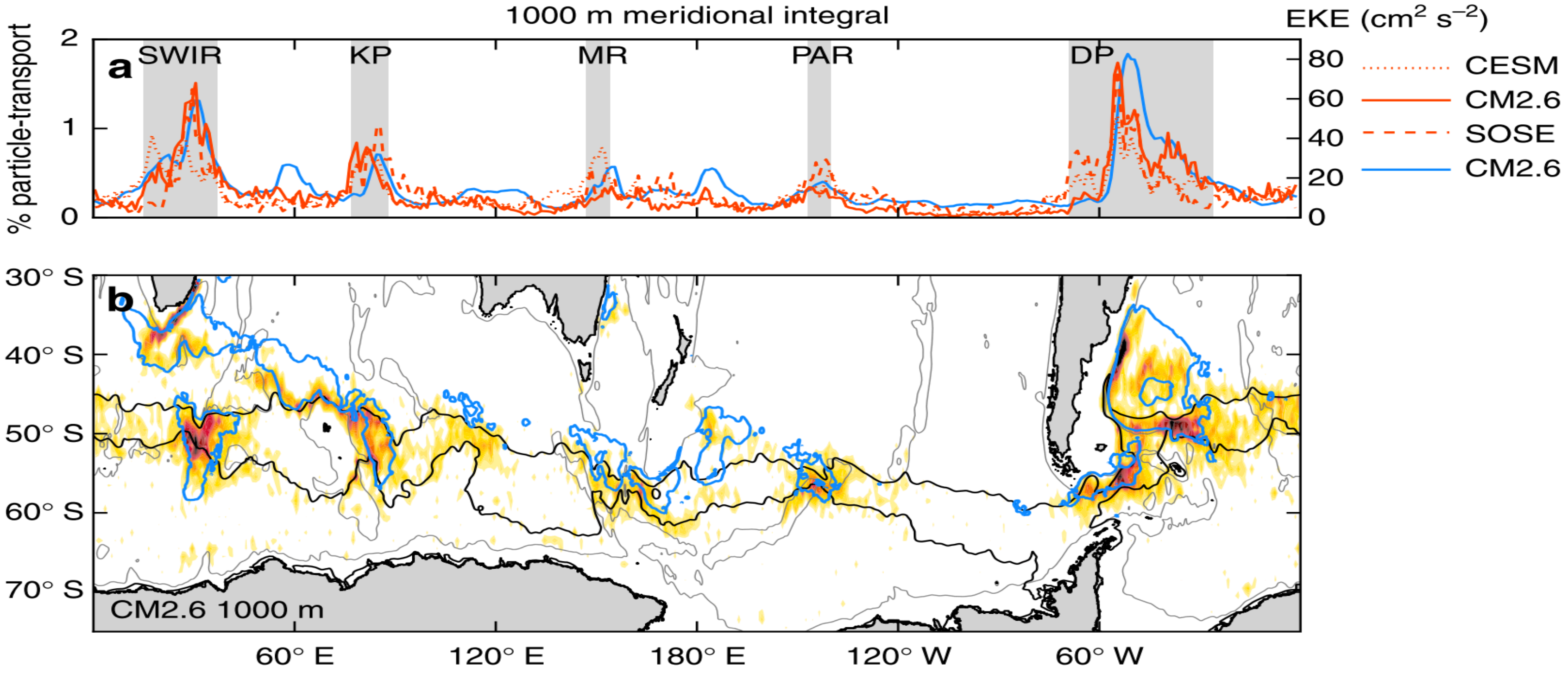

(Tamsitt et al, 2017)

EKE and upwelling near topography

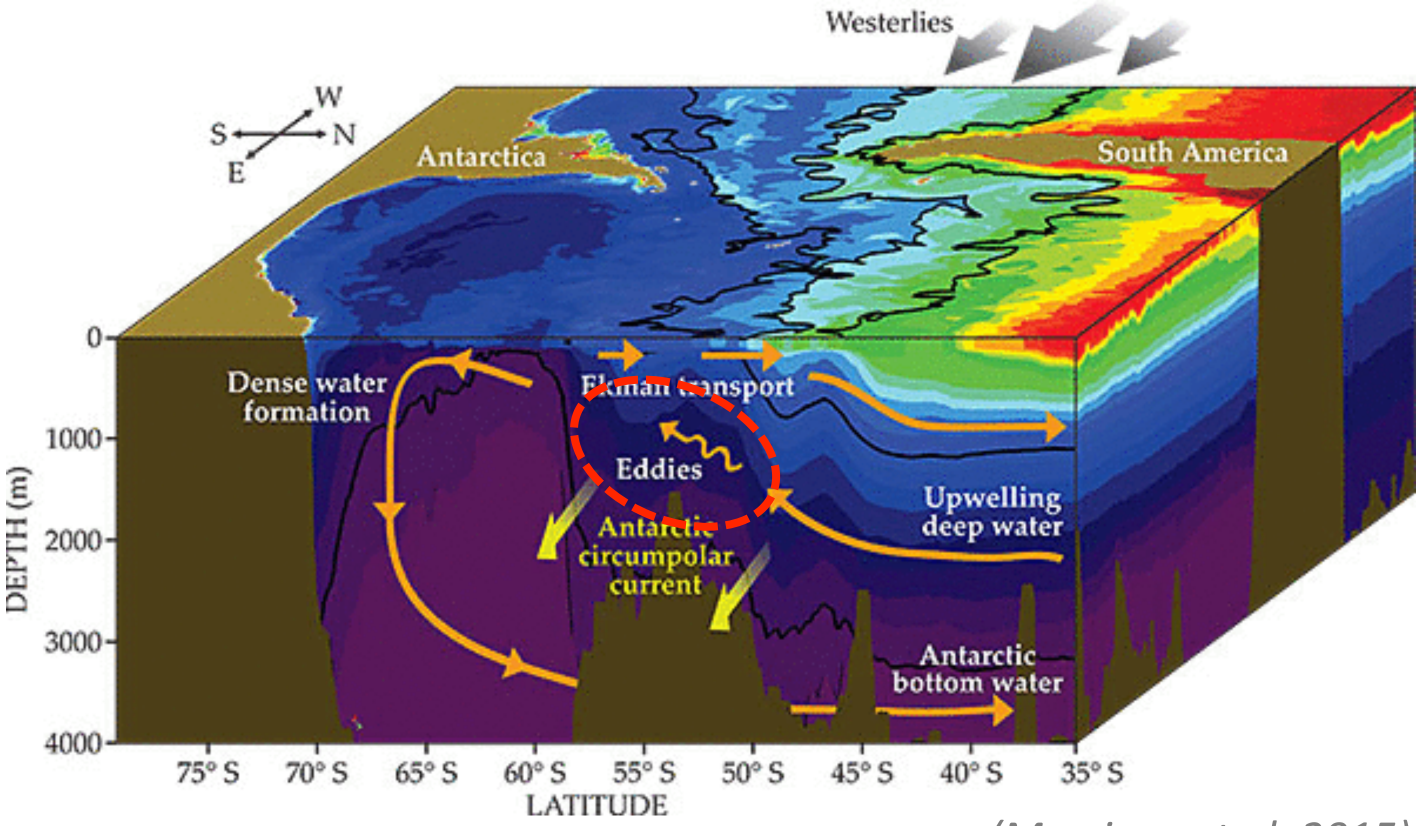

(Morrison et al, 2015)

Insights from idealized simulations

1. Impact of topography on eddy-driven isopycnal transport
   - Where?
   - Mechanism?
2. Relationship between (local) EKE and transport
   - Parameterizations?

Idealized model

- Adiabatic isopycnal model (MOM6)
- Two layers
- Inflowing jet
- Topography

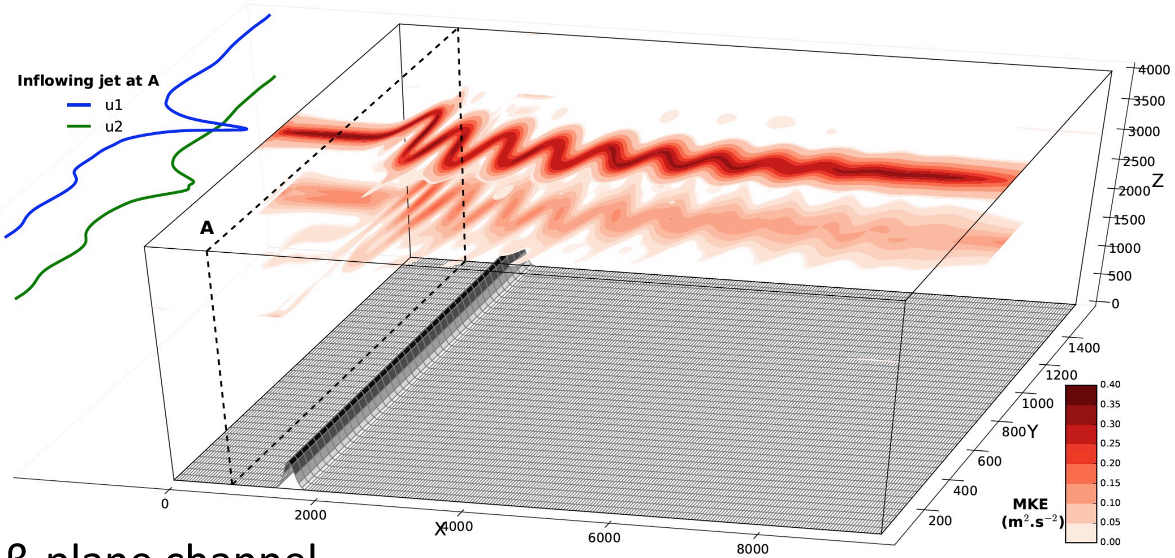

β-plane channel

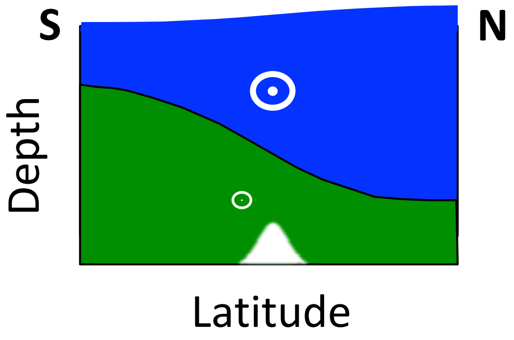

Idealized model

- **Adiabatic isopycnal model** (MOM6)
- Two layers
- Inflowing jet
- Topog

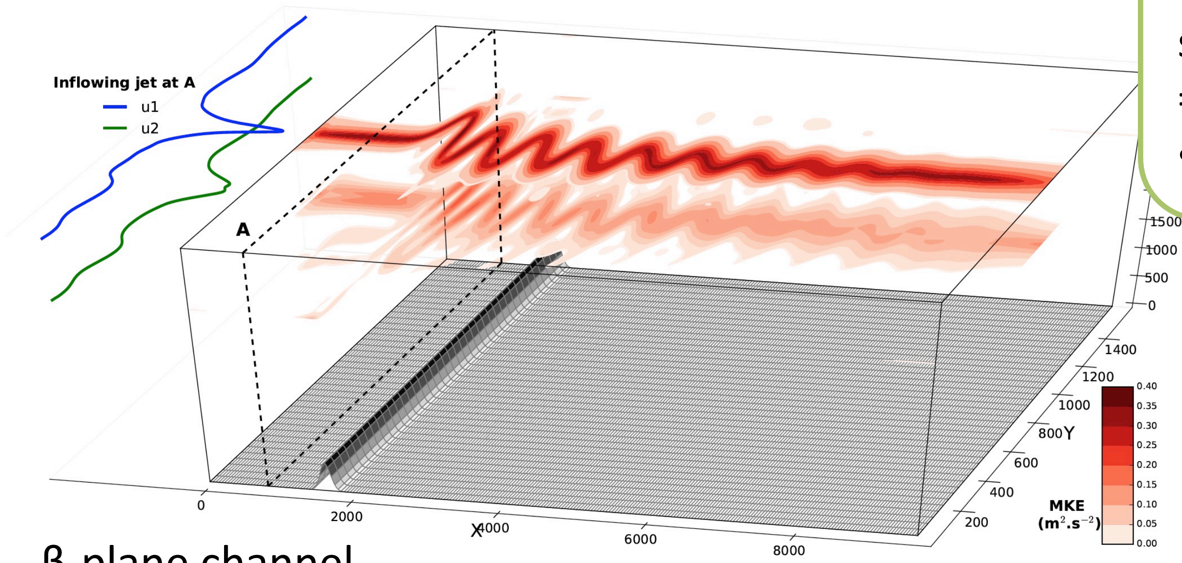

β-plane channel

- **'eddy upwelling'**

= cross-jet transport along southward-shoaling isopycnal = 'transient eddy' thickness flux

- Relevant for **mid-depth**

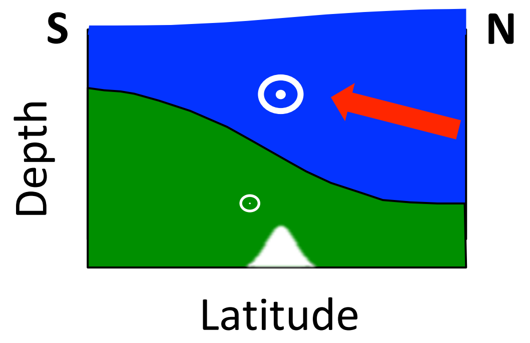

Idealized model

- Adiabatic isopycnal model
- **Two layers**

- Inflowing jet
- Top

- **Vertical and horizontal shear**
- Focus on **upper layer** (southward-shoaling)

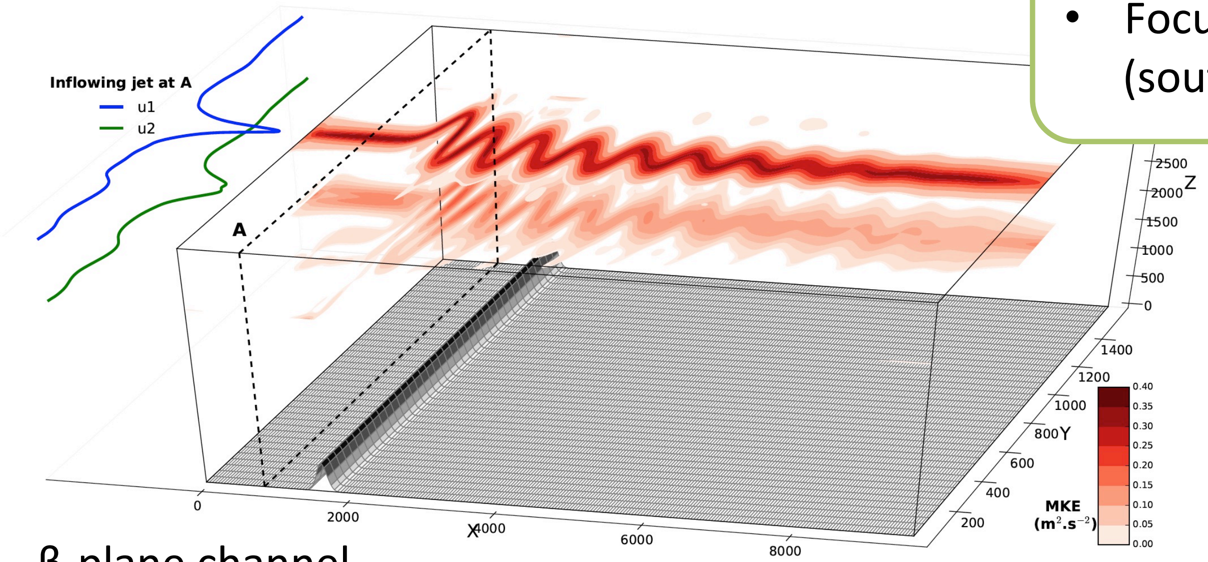

β-plane channel

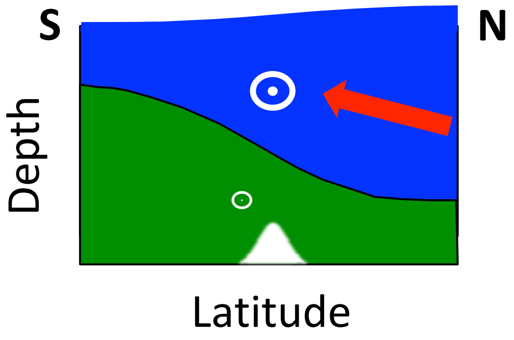

Idealized model

- Adiabatic isopycnal model
- Two layers
- **Inflowing jet**
- Topography

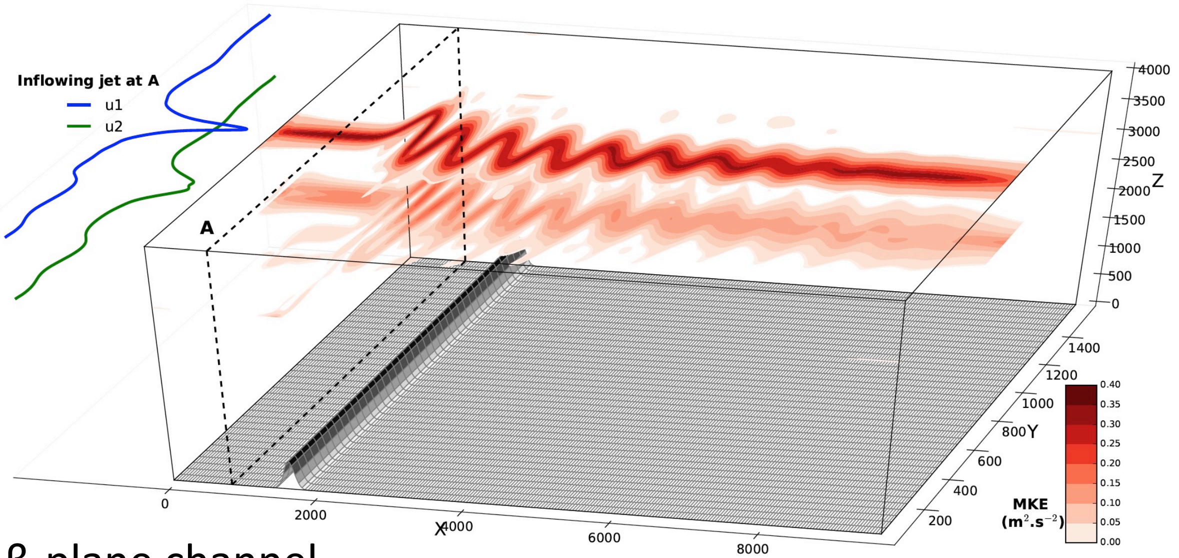

β-plane channel

- No local wind
- **Same inflow** with/ without topography

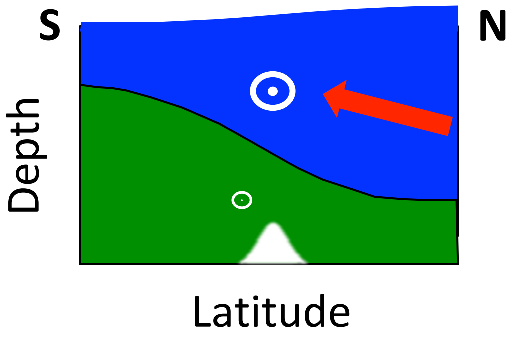

Idealized model

- Adiabatic isopycnal model
- Two layers
- **Inflowing jet**
- Topography

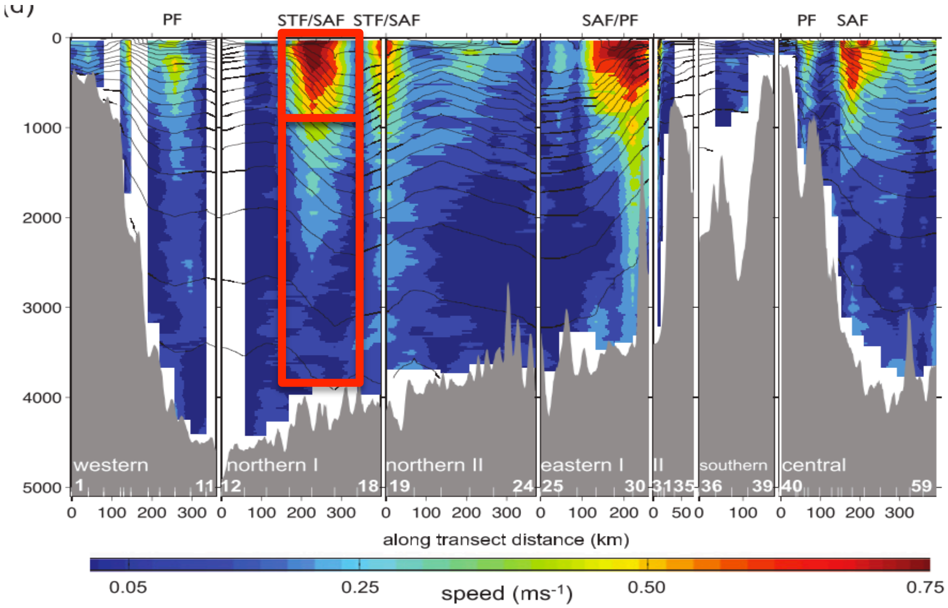

(Waterman et al., 2013)

Upper layer:
W = O(200 km)
D = 0-1000 m
U = O(0.8 m.s^{-1})

Lower layer:
W = O(200 km)
D = 1000-4000 m
U = O(0.2 m.s^{-1})

- No local wind
- **Same inflow** with/ without topography

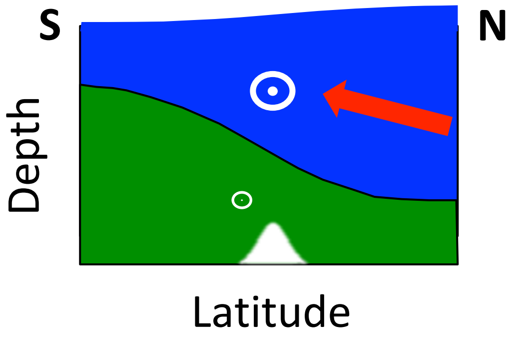

Idealized model

- Adiabatic isopycnal model
- Two layers
- Inflowing jet
- **Topography**

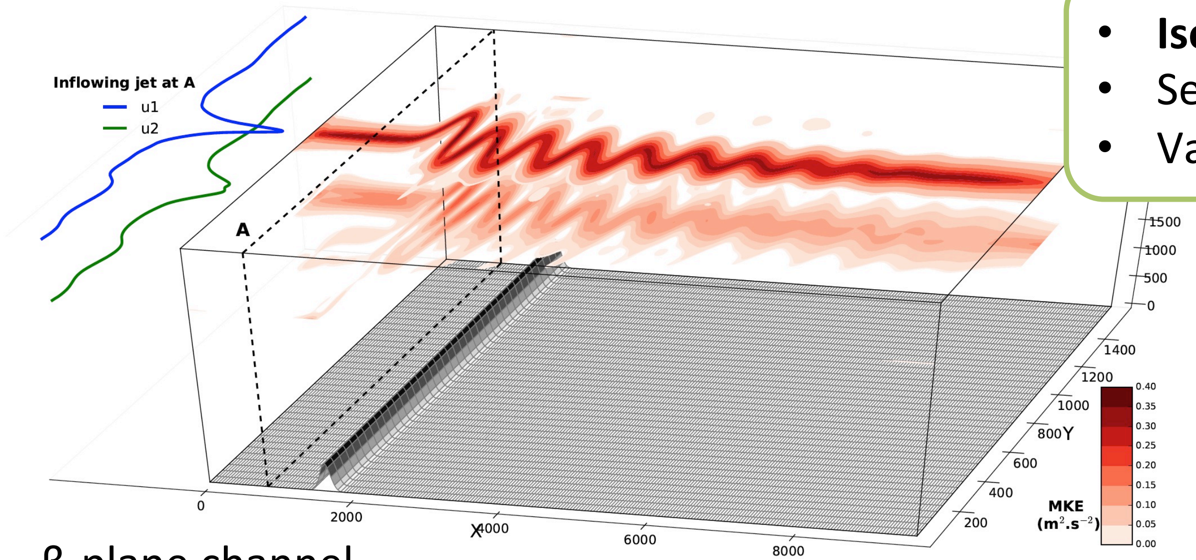

β-plane channel

- **Isolated** topography
- Seamount or meridional ridge
- Varying height

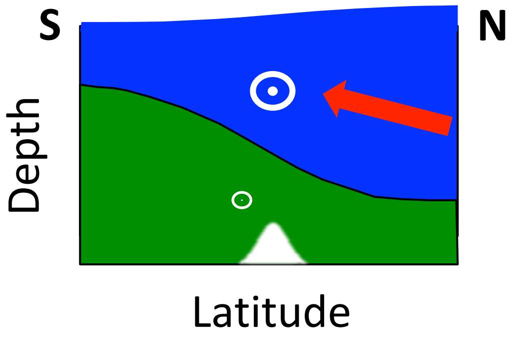

Impact of topography

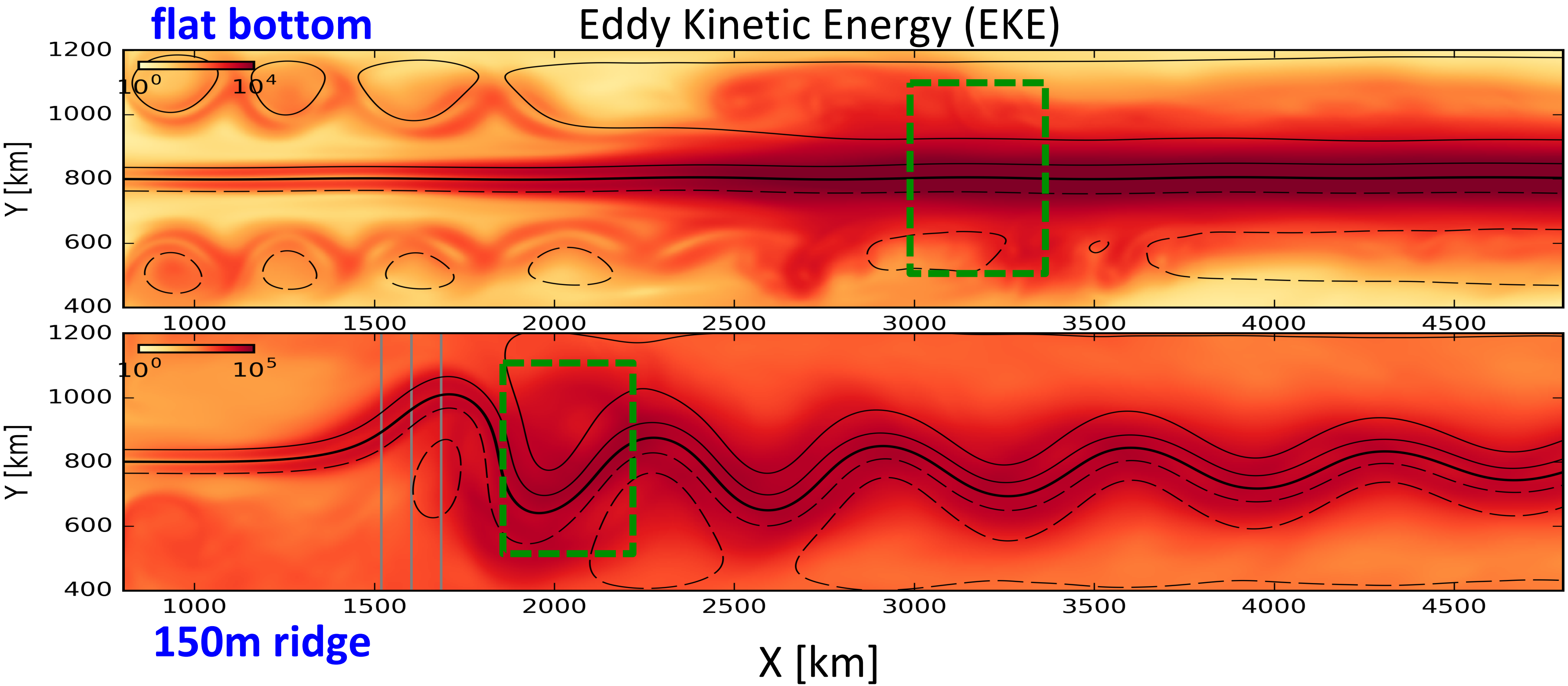

Impact of topography

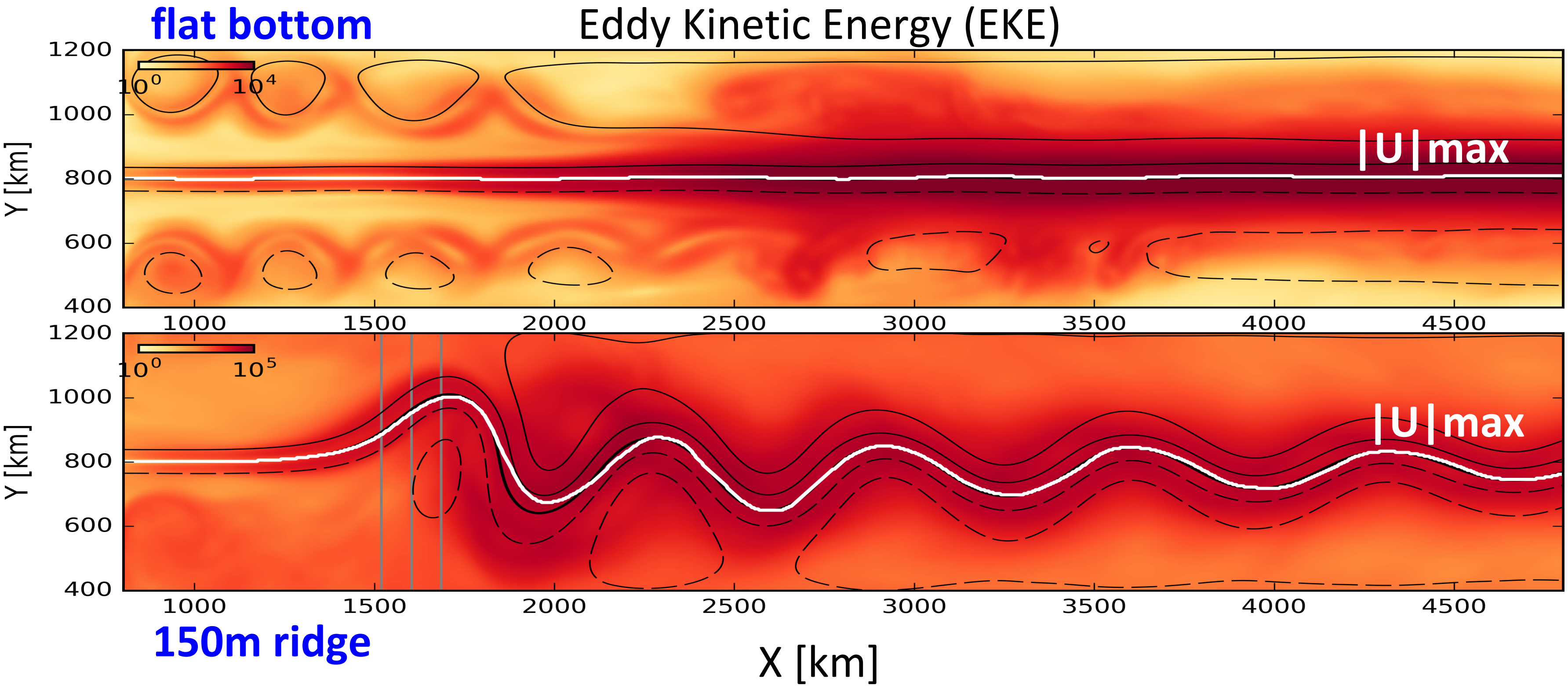

Impact of topography

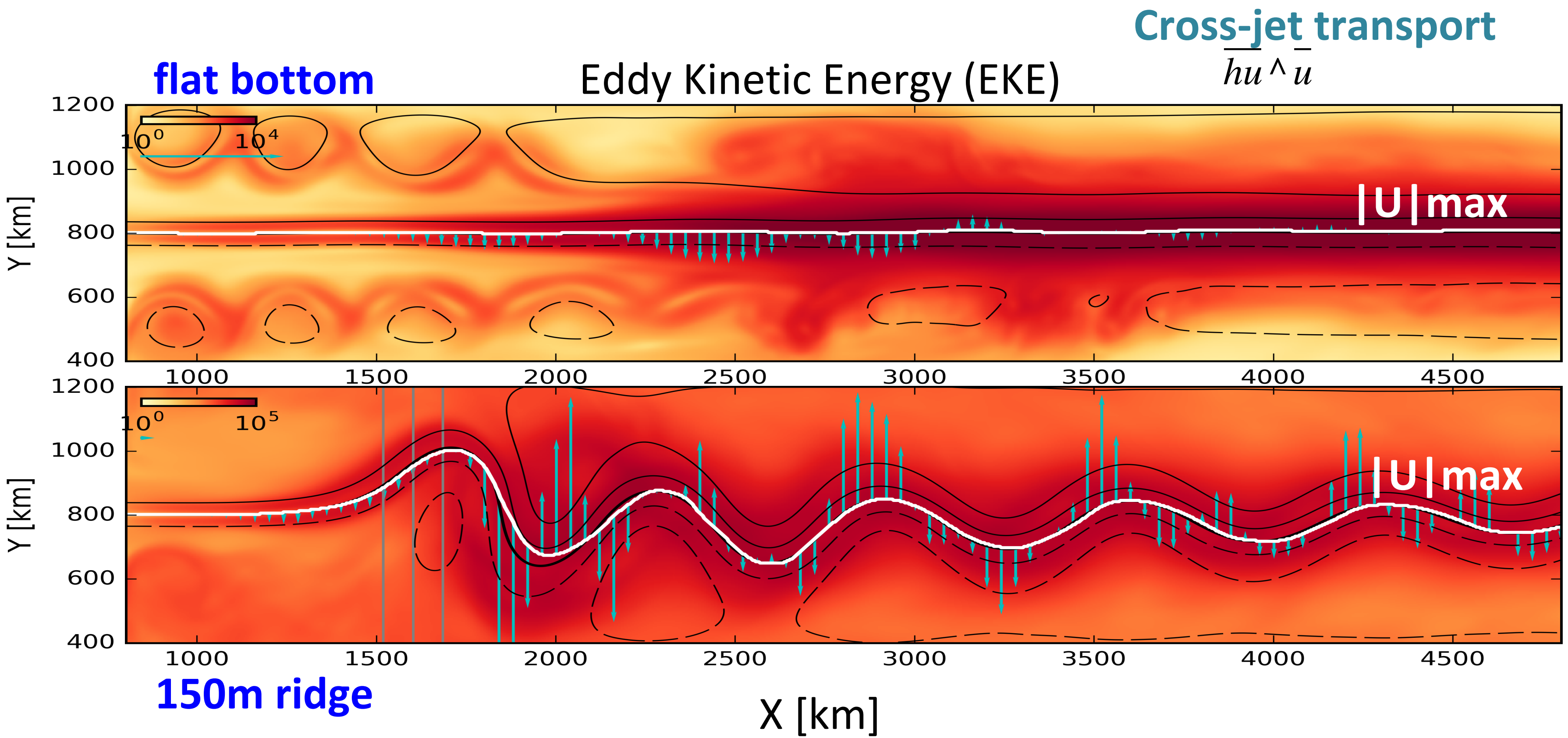

Impact of topography

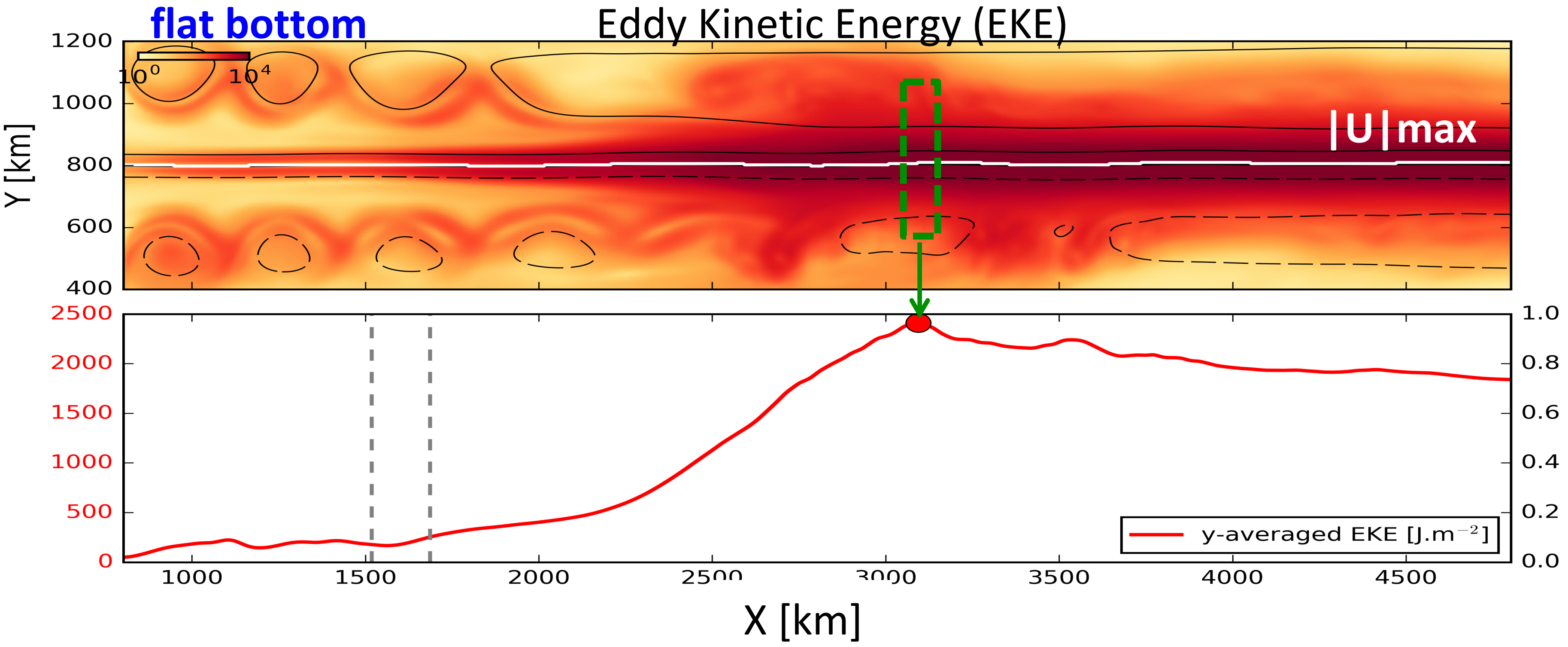

Impact of topography

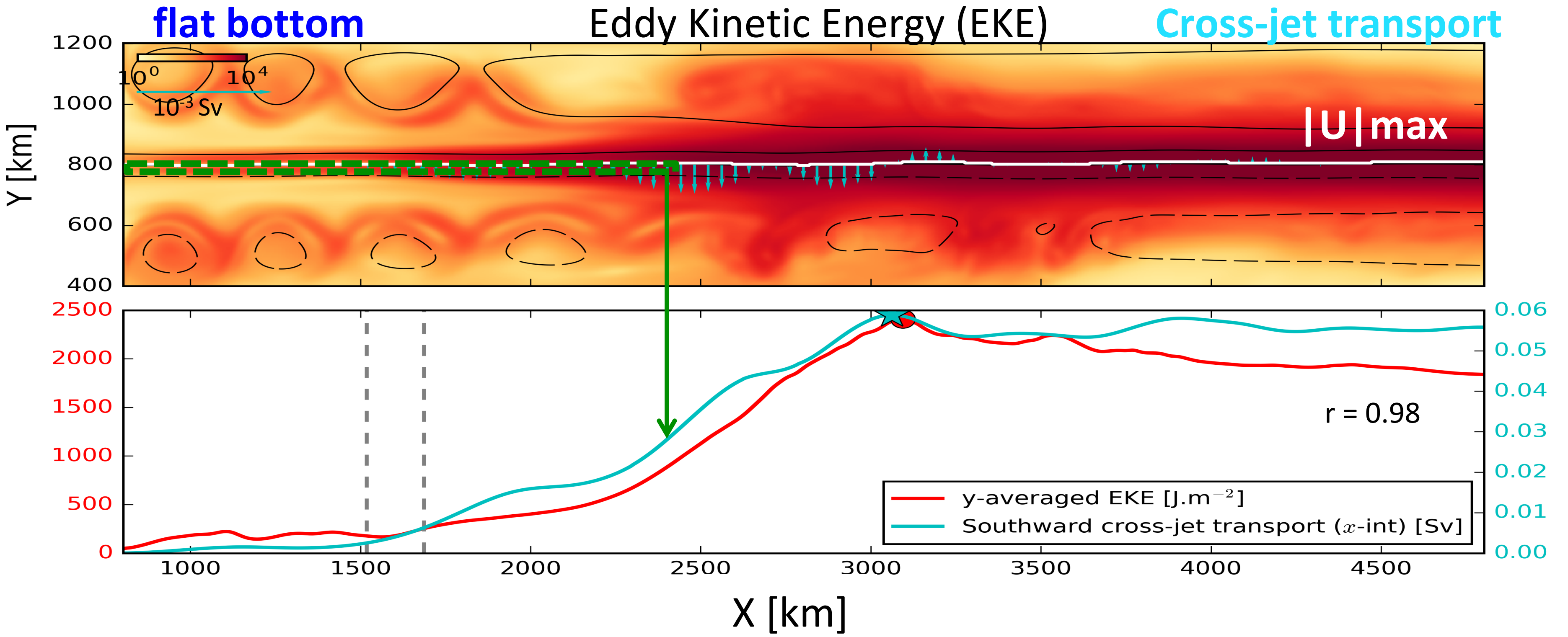

Impact of topography

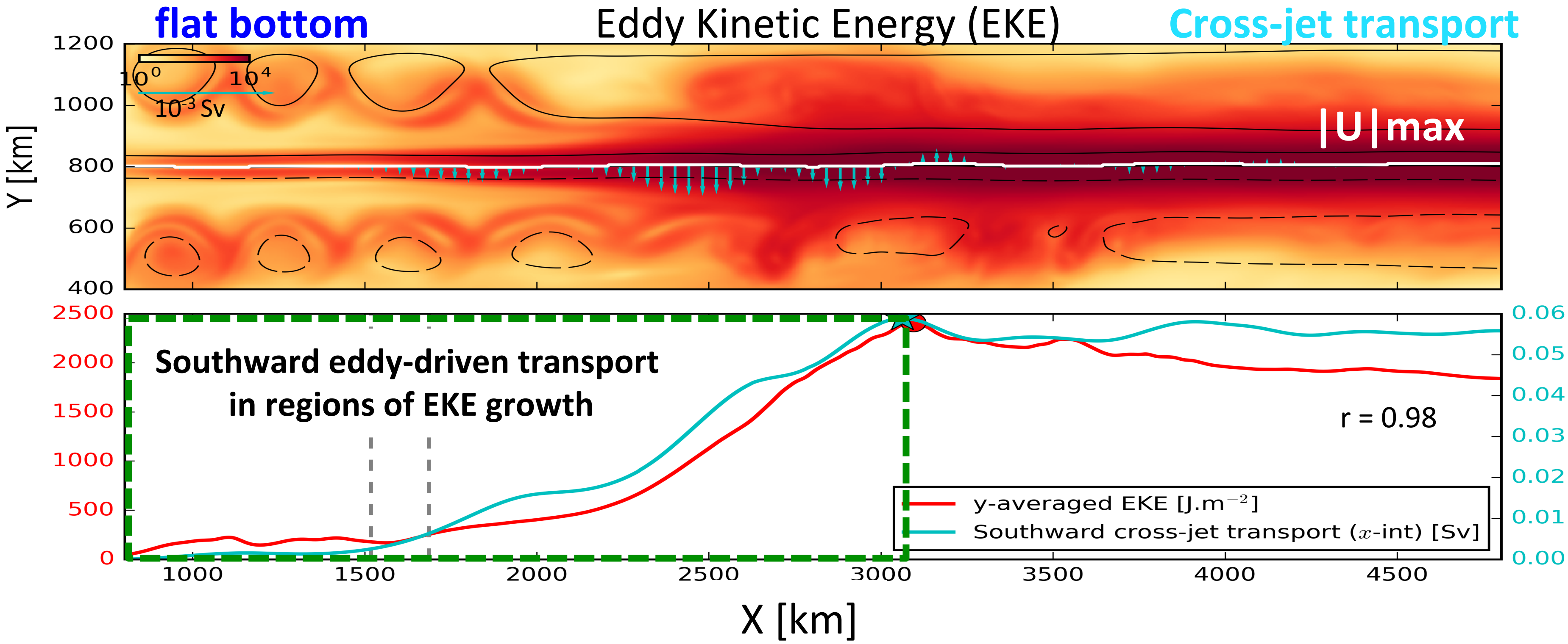

Impact of topography

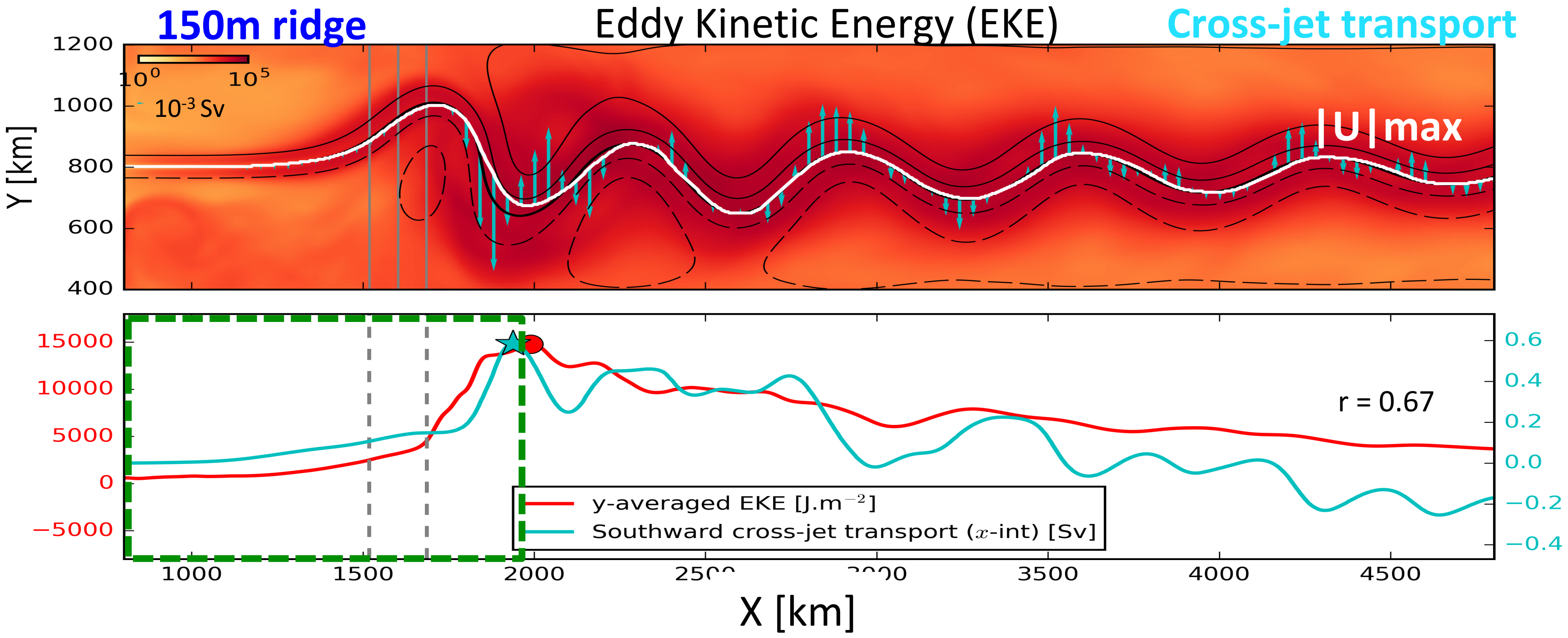

Insights from idealized simulations

1. Impact of topography on eddy-driven transport
   - **Enhanced and localized** transport downstream of topography
   - Magnitude and region extent vary with topography
2. Relationship between EKE and transport
   - Southward transport occurs in regions of **EKE growth** (not EKE maximum)

Insights from idealized simulations

1. Impact of topography on eddy-driven transport
   - **Enhanced and localized** transport downstream of topography
   - Magnitude and region extent vary with topography
2. Relationship between EKE and transport
   - Southward transport occurs in regions of **EKE growth** (not EKE maximum)

supports the findings of
(Tamsitt et al 2017;
Foppert et al 2017)

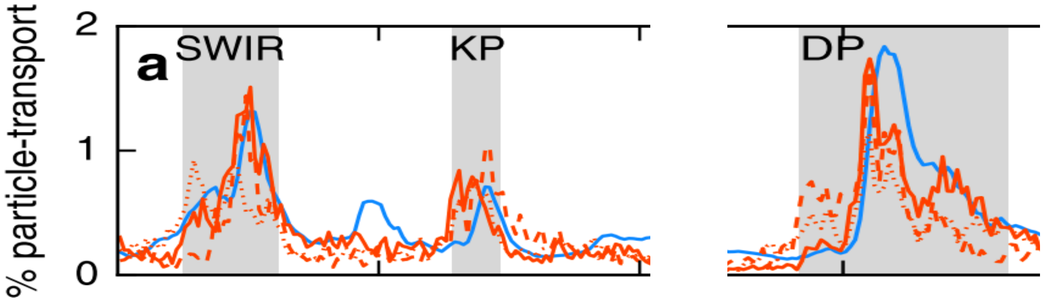

Exploring the mechanism

- Thickness-weighted energy budget:

$h = \overline{h} + h'$ time-mean + ‘eddies’

$u = \hat{u} + u''$ thickness-weighted mean + ‘eddies’

with $\hat{\mathbf{u}}_i \equiv \dfrac{\overline{h_i \mathbf{u}_i}}{\overline{h_i}}$.

$$\overline{KE_i} = \underbrace{\frac{\rho_0}{2}\overline{h_i}\left\|\hat{u}_i\right\|^2}_{\text{MKE}_i} + \underbrace{\frac{\rho_0}{2}\overline{h_i\left\|u_i''\right\|^2}}_{\text{EKE}_i}$$

Kinetic energy in layer *i*

$$\overline{APE_1} = \overline{\frac{\rho_0}{2}g'(\eta_1)^2} = \underbrace{\frac{\rho_0}{2}g'(\overline{\eta_1})^2}_{MAPE_1} + \underbrace{\frac{\rho_0}{2}g'\overline{\eta_1'^2}}_{EAPE_1},$$

Potential Energy

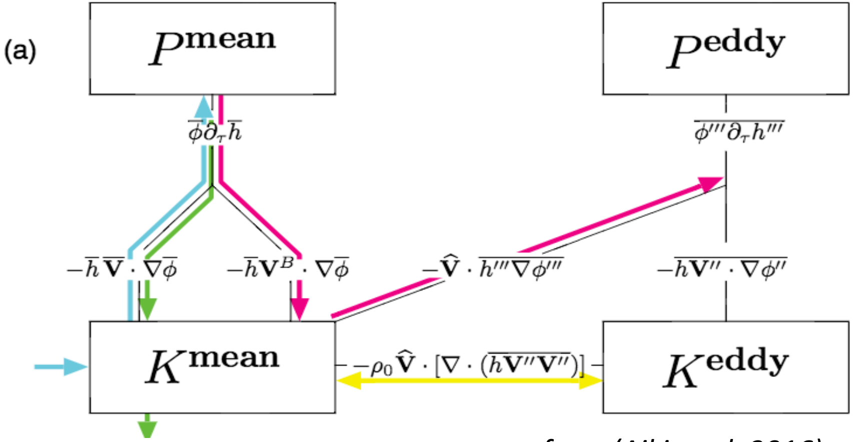

from (Aiki et al. 2016)

Bleck 1985; Aiki & Greatbatch 2012;
Aiki et al 2016; Ringler et al 2017;
Barthel et al 2017: Jet–Topography Interactions Affect Energy Pathways to the Deep Southern Ocean

Exploring the mechanism

- Thickness-weighted energy budget:

$h = \overline{h} + h'$ time-mean + 'eddies'

$u = \hat{u} + u''$ thickness-weighted mean + 'eddies'

with $\hat{\mathbf{u}}_i \equiv \dfrac{\overline{h_i \mathbf{u}_i}}{\overline{h_i}}$.

$$\overline{KE_i} = \underbrace{\frac{\rho_0}{2}\overline{h_i}\left\|\hat{u}_i\right\|^2}_{\mathbf{MKE_i}} + \underbrace{\frac{\rho_0}{2}\overline{h_i\left\|u_i''\right\|^2}}_{\mathbf{EKE_i}}$$

Kinetic energy in layer *i*

$$\overline{APE_1} = \overline{\frac{\rho_0}{2}g'(\eta_1)^2} = \underbrace{\frac{\rho_0}{2}g'(\overline{\eta_1})^2}_{MAPE_1} + \underbrace{\frac{\rho_0}{2}g'\overline{\eta_1'^2}}_{EAPE_1},$$

Potential Energy

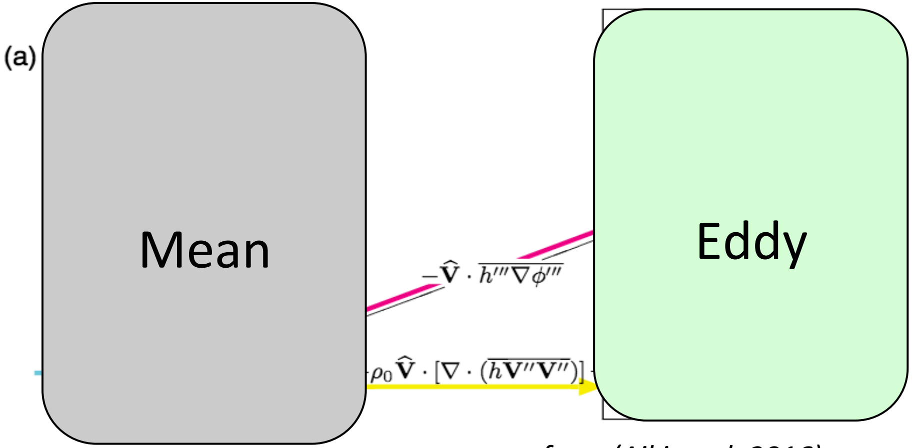

from (Aiki et al. 2016)

Bleck 1985; Aiki & Greatbatch 2012;
Aiki et al 2016; Ringler et al 2017;
Barthel et al 2017: Jet–Topography Interactions Affect Energy Pathways to the Deep Southern Ocean

Exploring the mechanism

- Thickness-weighted energy budget:

Two local eddy-mean conversion terms in the upper layer

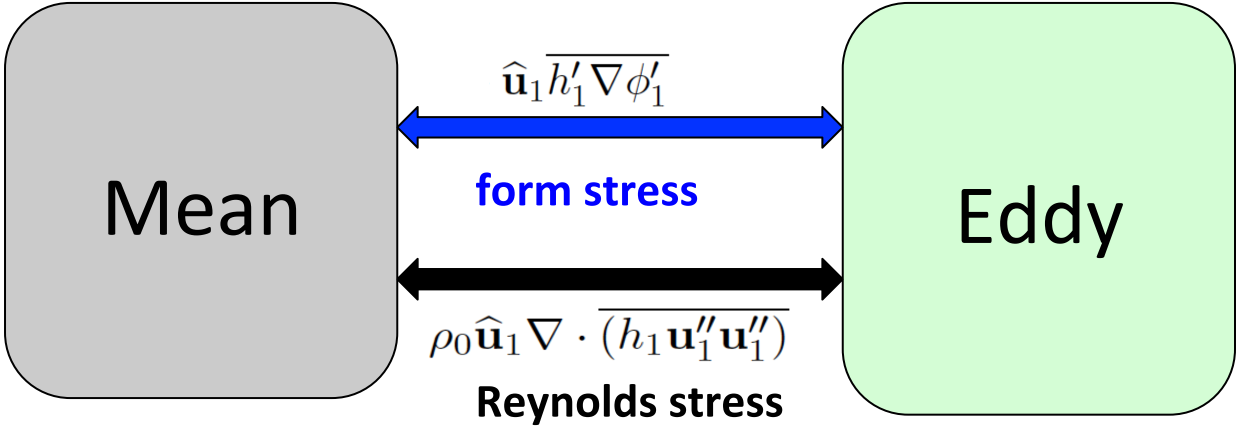

$h = \overline{h} + h'$ time-mean + 'eddies'

$u = \hat{u} + u''$ thickness-weighted mean + 'eddies'

'baroclinic';
'barotropic'

Exploring the mechanism

- A revealing case study:

most cases explored have similar zonal distributions for both eddy-mean energy conversion terms *(see Barthel et al 2017: Jet–Topography Interactions Affect Energy Pathways to the Deep Southern Ocean)*

the most revealing case is when they do not.

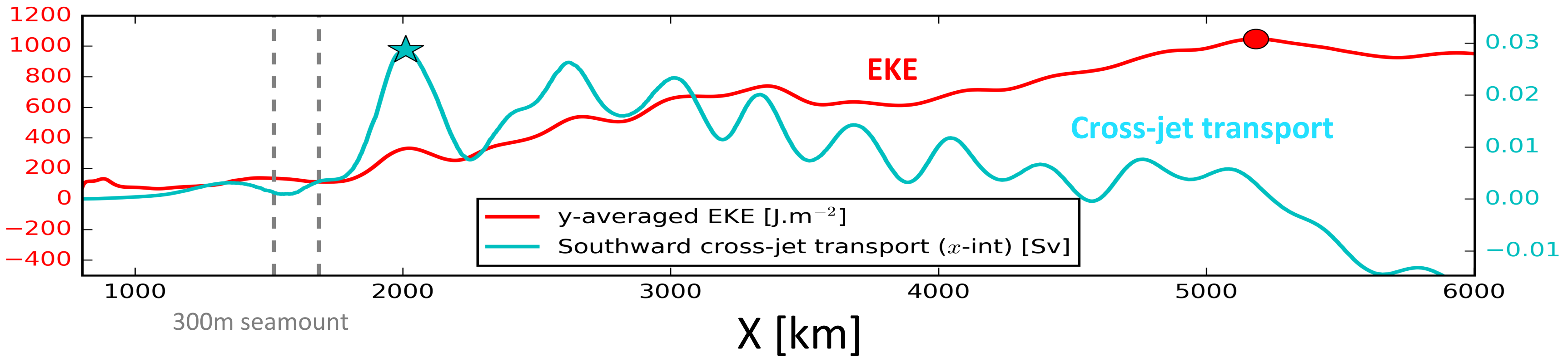

Exploring the mechanism

- A revealing case study:

EKE is generated through both 'baroclinic' and 'barotropic' instability.

Cross-jet transport occurs only where 'baroclinic' instability is acting.

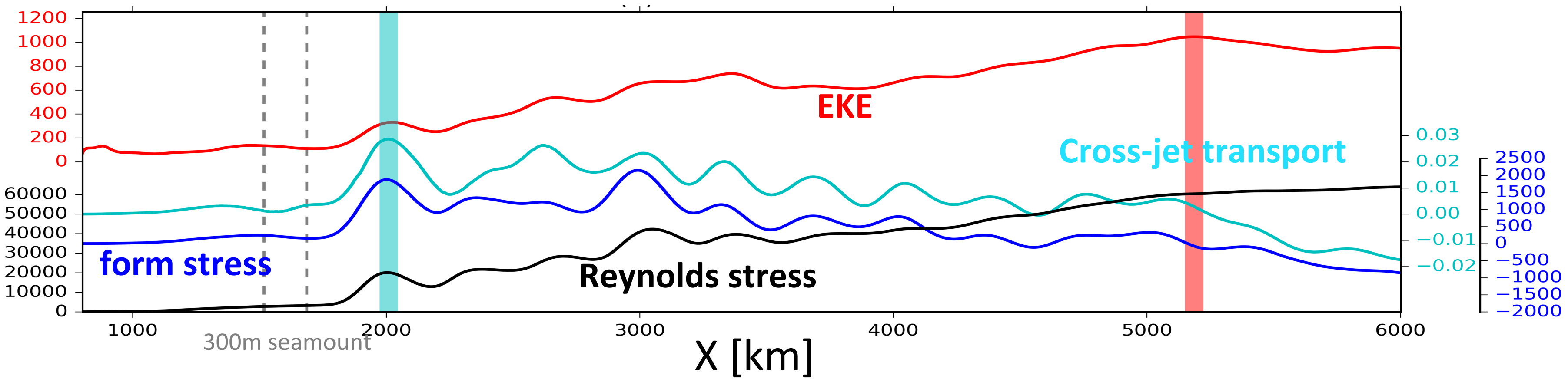

Energy conversion terms (form stress, Reynolds stress) plotted above are along-stream integrated, just like cross-jet transport. EKE is not.

Insights from idealized simulations

1. Impact of topography on eddy-driven transport
   - **Enhanced and localized** transport downstream of topography
   - Magnitude and region extent vary with topography
2. Relationship between EKE and transport
   - Southward transport occurs in regions of **EKE growth** through **baroclinic instability**

Exploring the mechanism

- Southward eddy-driven transport occur where baroclinic instability energizes the eddy field
- Consistent with its role in ‘flattening isopycnals’ – upstream of EKE max (≠ tracer) (Karsten et al, 2002)

- In most cases, zonal growth of EKE is a better predictor at the local scale for southward transport than other variables (EKE, S)

  → a linear parameterization exercise (!)

A (linear) parameterization exercise

Zonal distribution of EKE/S do not match that of transport:

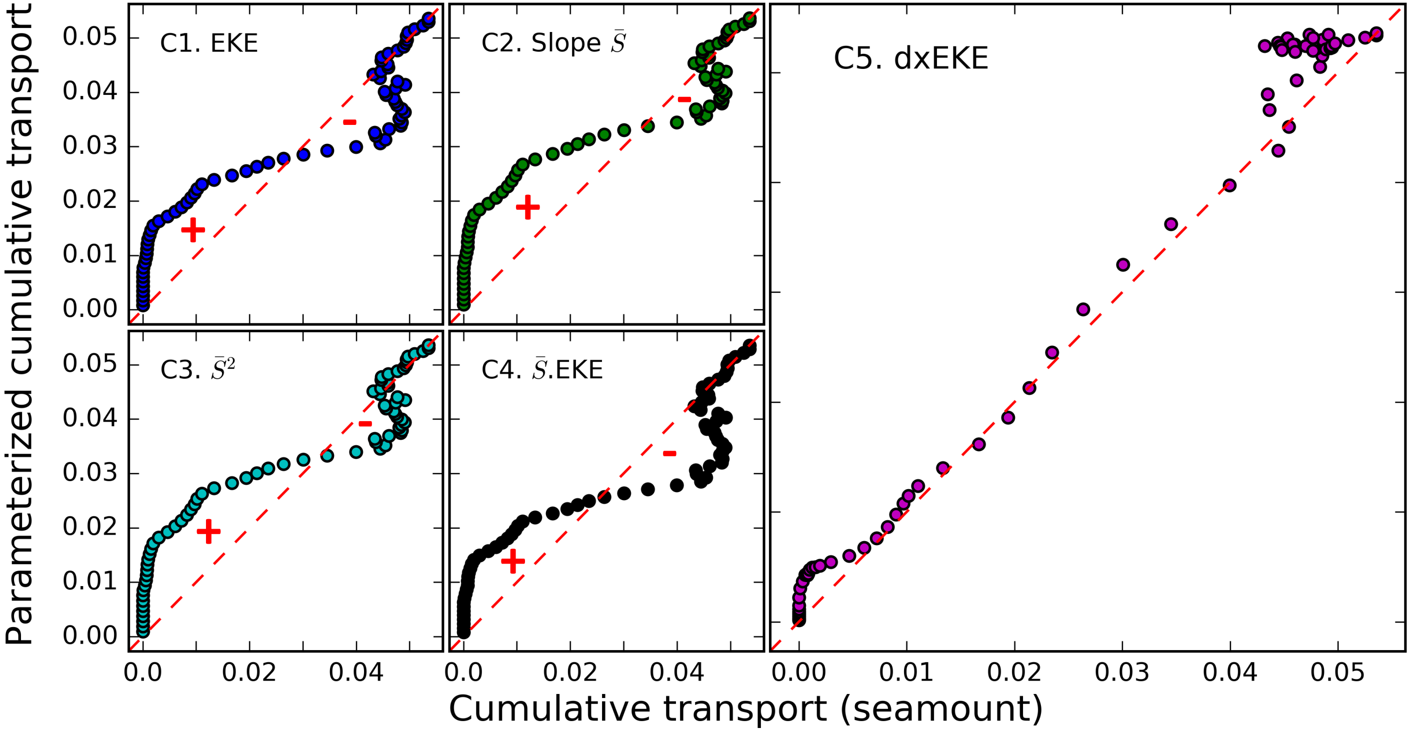

3-step Recipe

- 'coarsen' the variables (80km)
- find best linear fit (minimizing total error)
- compare parameterized transport to 'real' transport

A (linear) parameterization exercise

Zonal distribution of EKE/S do not match that of transport:

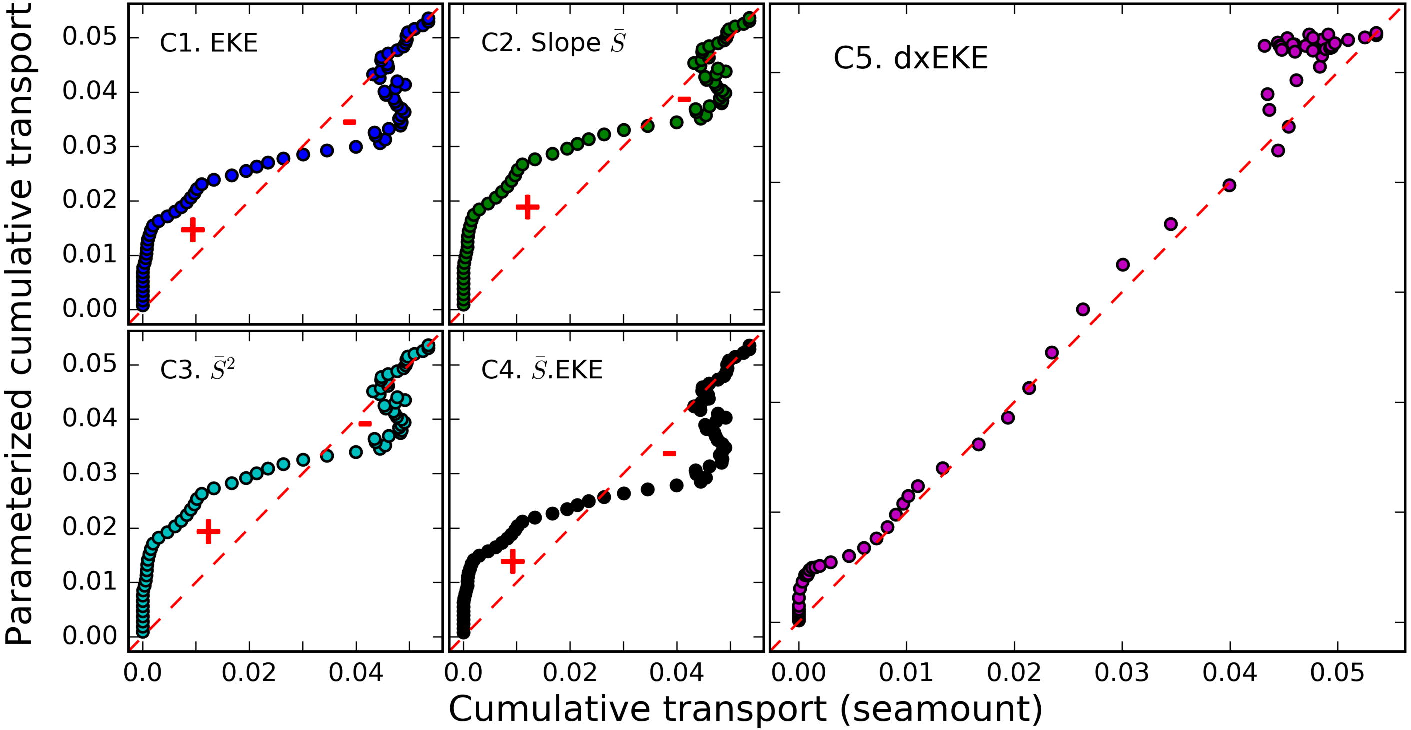

3-step Recipe

- 'coarsen' the variables (80km)
- find best linear fit (minimizing total error)
- compare parameterized transport to 'real' transport

BUT…

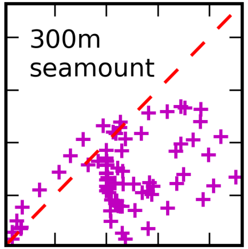

Summary

- The eddy-driven southward cross-jet transport is related to eddy-mean energy conversion through form stress (baroclinic instability).
  - may explain the spatial offset in *(Tamsitt et al, 2017)*
- Topography can enhance and localize the eddy-driven transport.
  - It does so by modifying the region of baroclinic growth
  - It also affects the response of transport to changes in upstream flow.
- EKE zonal growth is a better indicator of local southward transport (in most cases) than local EKE/S. But parameterizations should ultimately take into account the role of baroclinic instability.

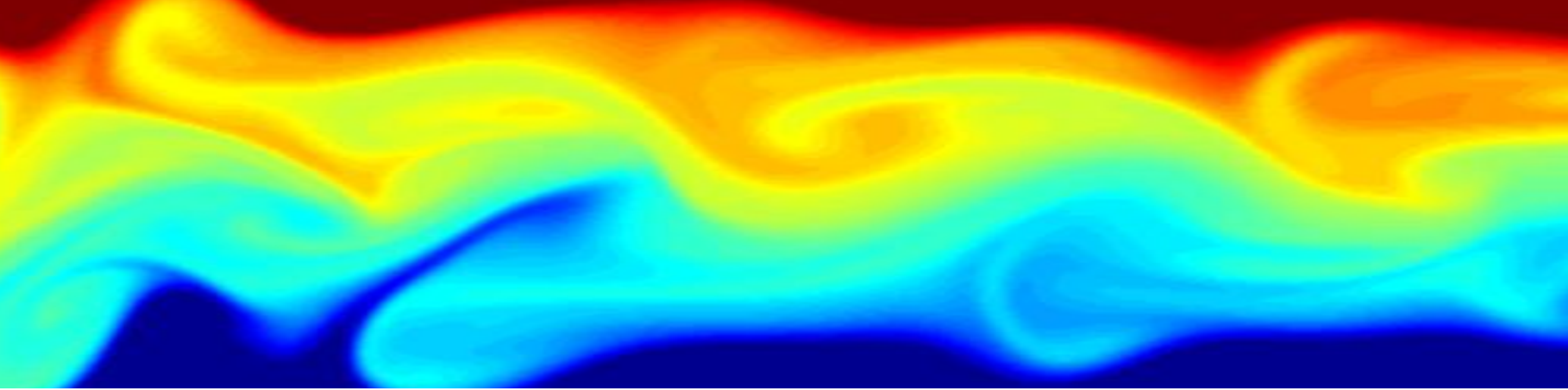

Thank you for your attention.
Questions?

abarthel@lanl.gov

Enhanced Eddy Kinetic Energy

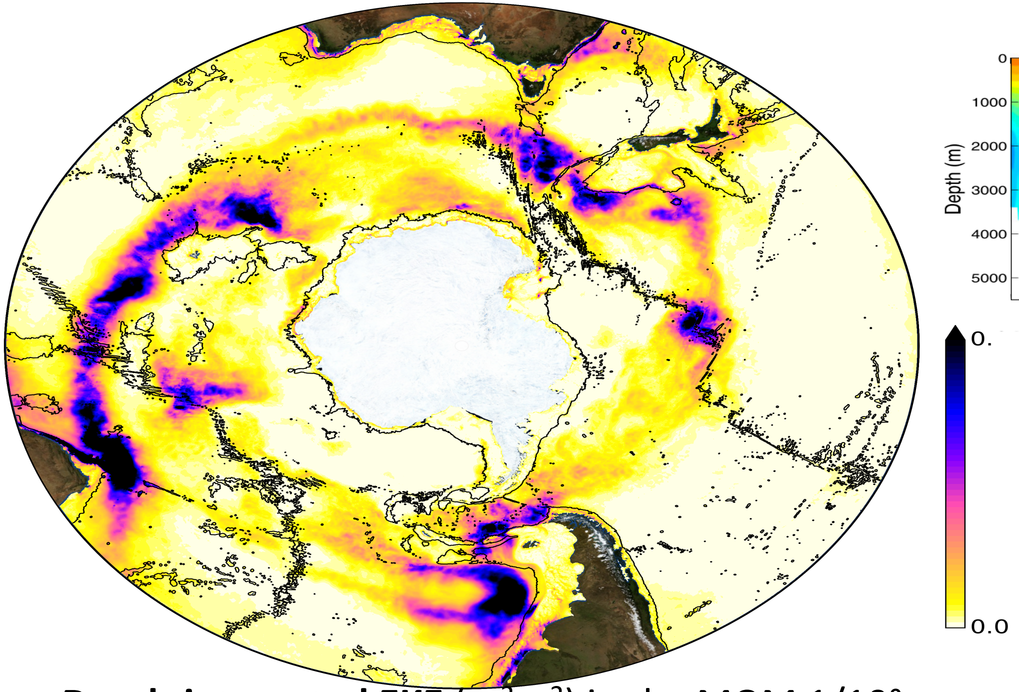

Depth-integrated EKE (m^2 s^{-2}) in the MOM 1/10° with the 2500m depth contour superimposed. Courtesy of Kial Stewart.

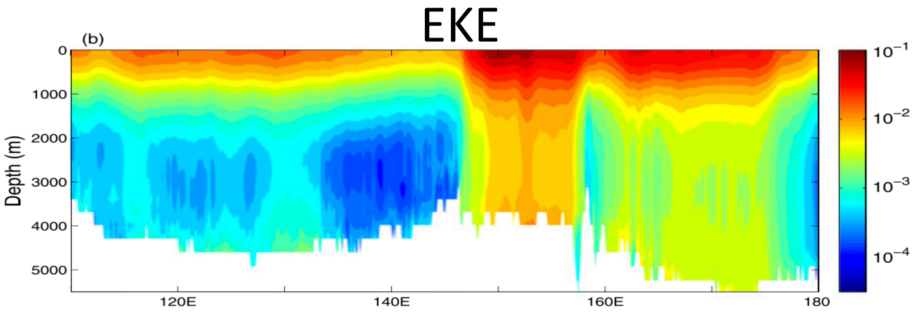

(Thompson and Naveira Garabato, 2013)

Energetics diagram

Aiki, H., X. Zhai, and R. J. Greatbatch,

Energetics of the global ocean: The role of mesoscale eddies, Chapter 4 in *The Indo-Pacific Climate Variability and Predictability*, edited by T. Yamagata and S. Behera, in press.

Fig. 2.

(a) in density coordinates

(b) in z coordinates

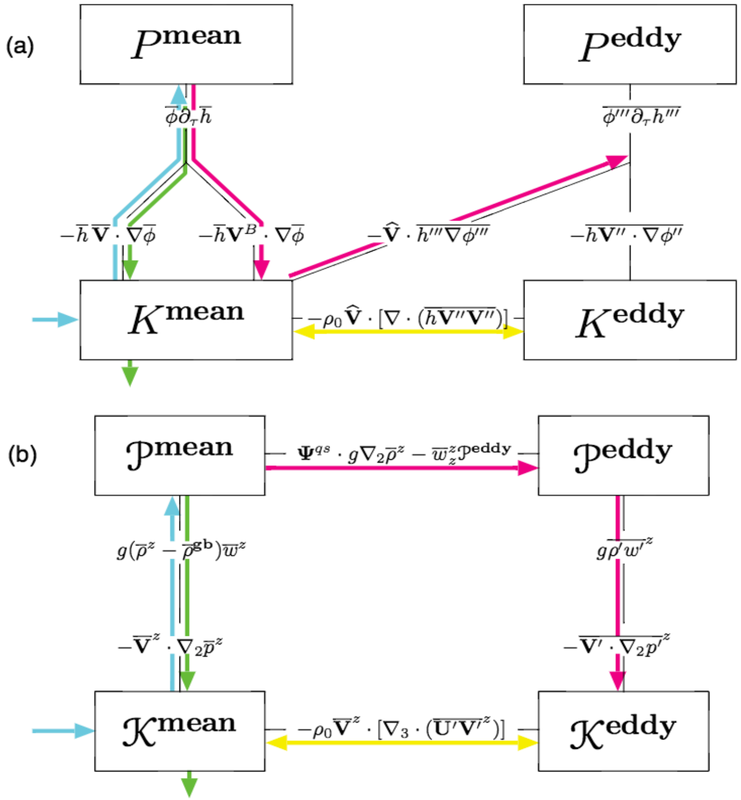

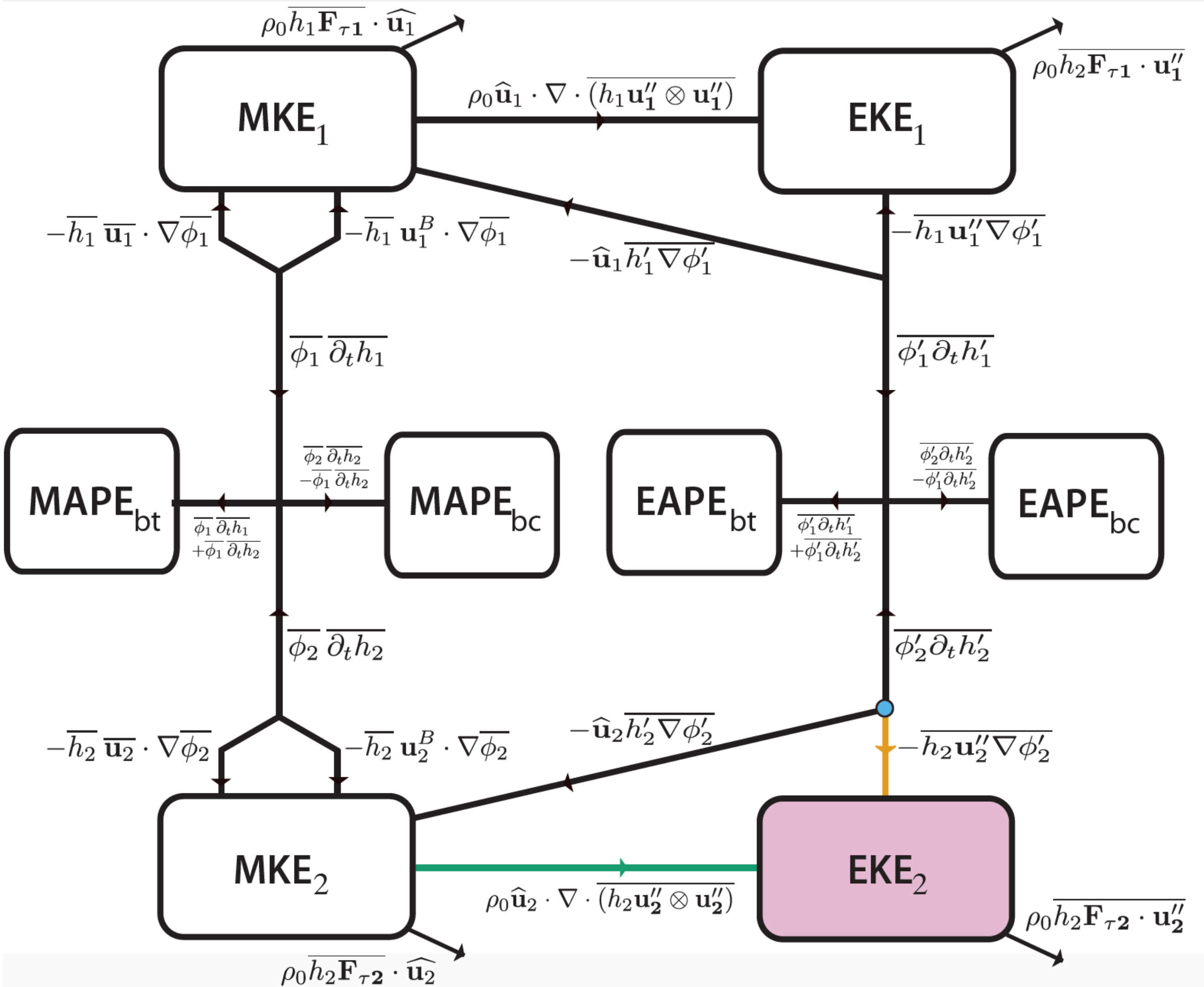

$$\overline{APE_0} = \overline{\frac{\rho_0}{2} g\eta_0{}^2} = \underbrace{\frac{\rho_0}{2} g\overline{\eta_0}^2}_{MAPE_0} + \underbrace{\frac{\rho_0}{2} g\overline{\eta_0'^2}}_{EAPE_0},$$

$$\overline{APE_1} = \overline{\frac{\rho_0}{2} g'(\eta_1)^2} = \underbrace{\frac{\rho_0}{2} g'(\overline{\eta_1})^2}_{MAPE_1} + \underbrace{\frac{\rho_0}{2} g'\overline{\eta_1'^2}}_{EAPE_1},$$

$$\overline{KE_i} = \overline{\frac{\rho_0}{2} h_i|\mathbf{u}_i|^2} = \underbrace{\frac{\rho_0}{2}\overline{h_i}\|\widehat{\mathbf{u}}_i\|^2}_{MKE_i} + \underbrace{\frac{\rho_0}{2}\overline{h_i\|\mathbf{u}_i''\|^2}}_{EKE_i}$$

3) Topography affects the response of the eddy isopycnal transport

Wind changes → baroclinic structure of ACC jets (*Langlais et al, 2015)*

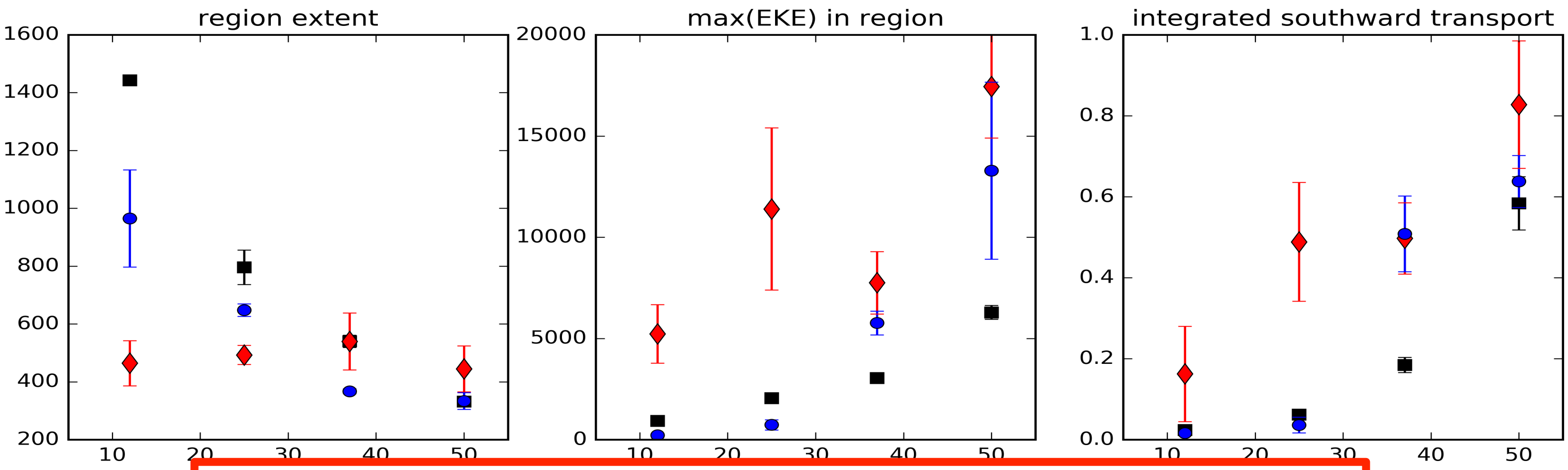

more baroclinic jet =
intensified localized transport

Sensitivity of the eddy upwelling depends on topography!

parameterizations

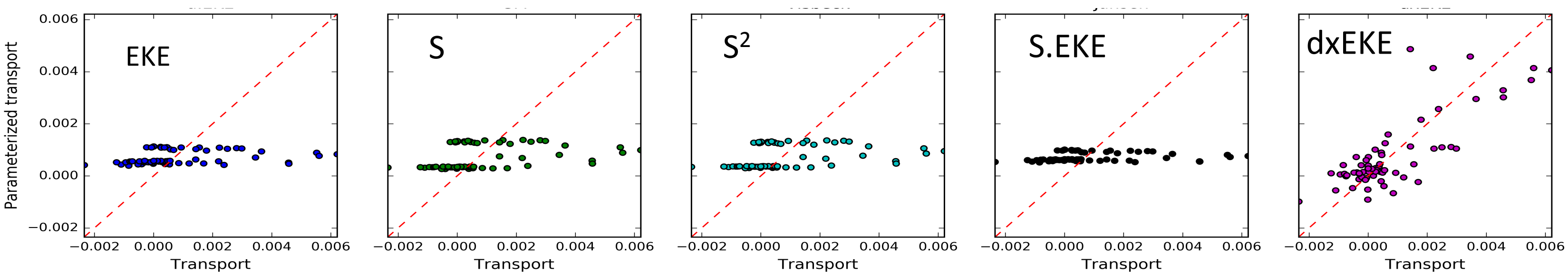

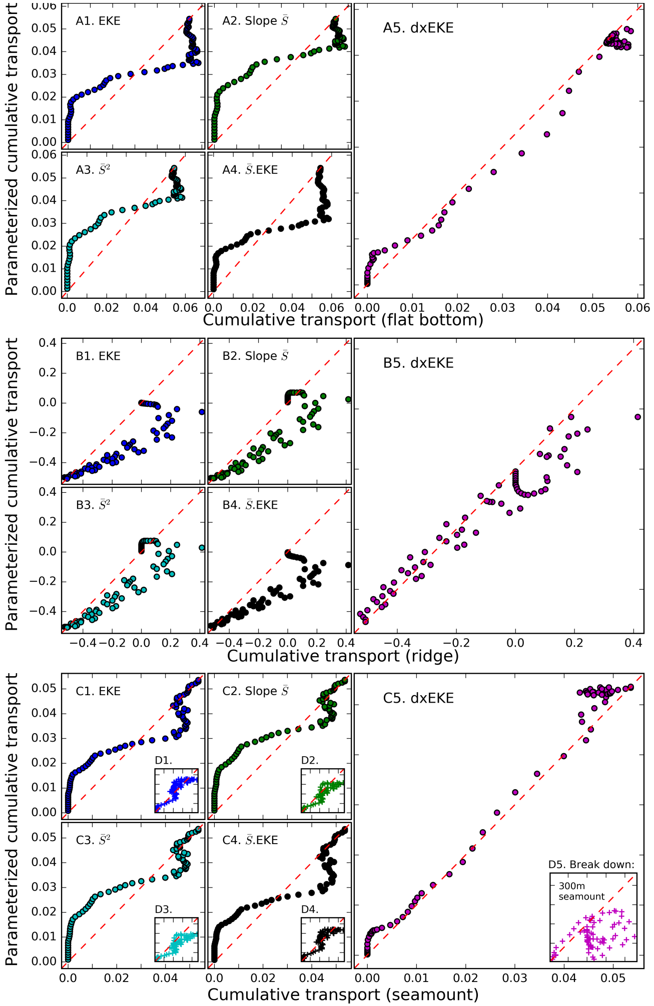

A1. EKE
A2. Slope $\bar{S}$
A3. $\bar{S}^2$
A4. $\bar{S}$.EKE
A5. dxEKE
Parameterized cumulative transport
Cumulative transport (flat bottom)
B1. EKE
B2. Slope $\bar{S}$
B3. $\bar{S}^2$
B4. $\bar{S}$.EKE
B5. dxEKE
Parameterized cumulative transport
Cumulative transport (ridge)
C1. EKE
C2. Slope $\bar{S}$
C3. $\bar{S}^2$
C4. $\bar{S}$.EKE
C5. dxEKE
D1.
D2.
D3.
D4.
D5. Break down:
300m
seamount
Parameterized cumulative transport
Cumulative transport (seamount)

References

- Aiki, H., X. Zhai, and R. J. Greatbatch, Energetics of the global ocean: The role of mesoscale eddies, Chapter 4 in *The Indo-Pacific Climate Variability and Predictability*, edited by T. Yamagata and S. Behera, World Scientific Publisher, in press.
- Nikurashin, M., Vallis, G., Adcroft, A. Routes to energy dissipation for geostrophic flows in the Southern Ocean, *Nature Geoscience*, 6, 48-51 (2013)
- K. L. Sheen, K. L., A. C. Naveira Garabato, J. A. Brearley, M. P. Meredith, K. L. Polzin, D. A. Smeed, A. Forryan, B. A. King, J-B. Sallée, L. St. Laurent, A. M. Thurnherr, J. M. Toole, S. N. Waterman, A. J. Watson. (2014). Eddy-induced variability in Southern Ocean abyssal mixing on climatic timescales. Nature Geoscience.577-582
- Thompson, A. F., and Richards, K. J. (2011). Low frequency variability of Southern Ocean jets. *Journal of Geophysical Research*, *116*(C9), C09022.

4) Toward parameterization

- First choice: form stress
- Second choice: dxEKE

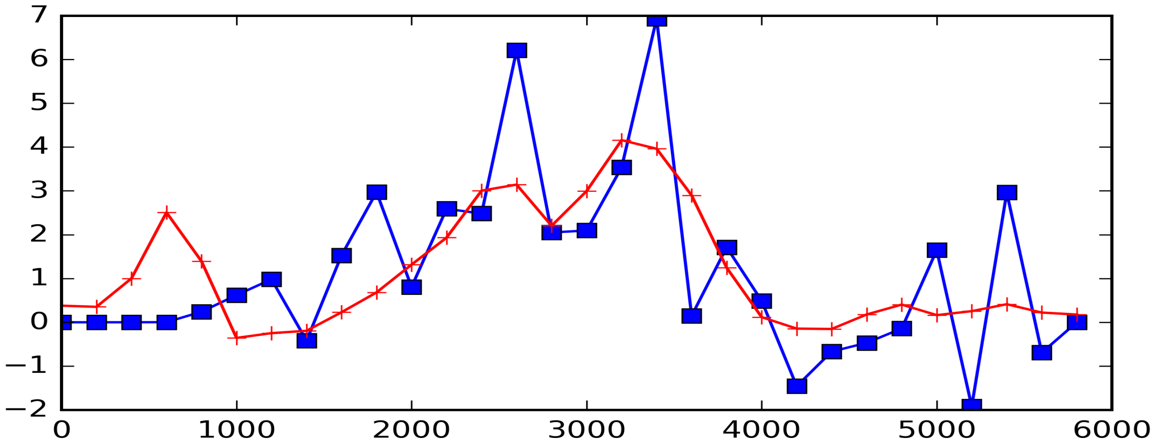

var	correlation	p-value
dxEKE	67 %	$4.\ 10^{-5}$
EKE	-9.7 %	0.61
S	25 %	0.18
S^2	24.7 %	0.18
S. EKE	-5.7 %	0.76

4) Toward parameterization

- First choice: form stress
- Second choice: dxEKE

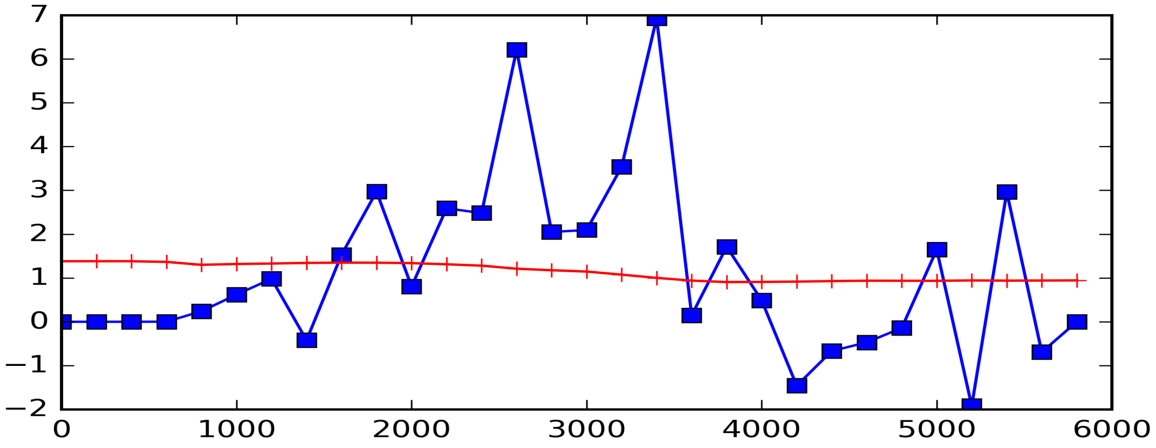

var	correlation	p-value
dxEKE	67 %	$4.\ 10^{-5}$
EKE	-9.7%	.61
S	25 %	0.18

2-layer isopycnal model

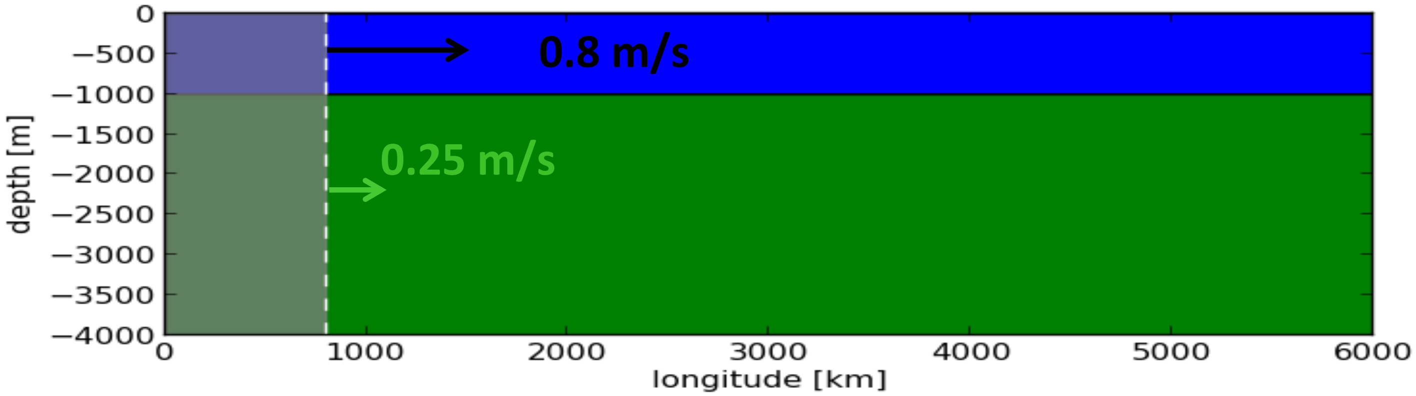

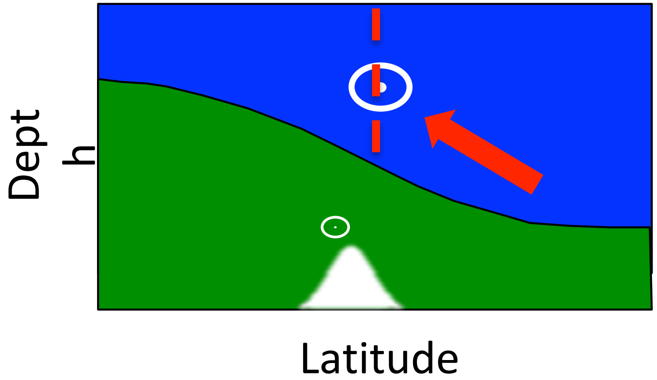

β-plane channel

eastward jet

metrics: EKE

eddy transport

controls: inflow

topography

depth [m]

Model parameters

- Bottom drag law c_drag*|u|*u, with c_drag = 5.0E-04
- Barotropic – baroclinic split: DT=120.0
- Biharmonic horizontal viscosity: AH = 1.5E+09
- Beta plane: BETA = 1.5E-11